3.1 TEN YEARS OF HIGH-RESOLUTION SEA SURFACE TEMPERATURES - WHAT HAVE WE LEARNED?

Michael J. Uddstrom*
National Institute of Water and Atmospheric Research, Wellington, New Zealand

1 INTRODUCTION

The NIWA Sea surface temperature Archive (NSA) dataset provides 1.1 km resolution coverage of the southwest Pacific Ocean region – an area of considerable oceanographic complexity. Data are available for the period 1 January 1993 to the present. Uddstrom and Oien (1999) (henceforth UO) used the first five years of these data to derive a climatology for the region, and employed empirical orthogonal function (EOF) decomposition of seasonal and monthly anomalies to specify the spatial and temporal variability of surface-visible ocean features. This was the first analysis of this type for the region, and the results suggested a number of potentially testable hypotheses, some of which contradicted conventional understanding at the time. Principal among these were the conjectures that there is only one subtropical front (STF) east of New Zealand, that it is locked to the southern edge of the Chatham Rise (CR), and that east of the CR, the STF dips south to lie near 47°S on the dateline, just north of the sub Antarctic Front (SAF) (see Figure 6 in UO). The UO analysis also suggested that some water masses appeared to display distinct signatures in SST annual cycle amplitude.

Now that the NSA contains 10 years of data it is possible to review some of these hypotheses, describe the inter-annual variability more completely, report on the impact of the anomalous El Niño event of 1998 on the New Zealand region, review the SST trends reported by Strong et al. (2000) and Casey and Cornillon (2001) in the light of the NSA data record, and compare the NSA data with those derived by the Pathfinder project.

2 THE DATA

2.1 NSA

The NSA data are derived from local area coverage Advanced Very High Resolution Radiometer (AVHRR) observations from NOAAs 11, 12, 14, 15, 16 and 17. The same radiometric calibration and 3 × 3 instantaneous field of view (ifov) resolution Bayesian cloud detection algorithms (Uddstrom *et al.*, 1999) have been used throughout the period, and SSTs are retrieved using the NOAA/NESDIS split-window Non Linear SST (NLSST) algorithm, where the first guess surface temperature is provided by the equivalent multi-channel algorithm. After retrieval the data are mapped onto a 3504 × 3504 pixel Lambert Conformal map projection, yielding up to 8 sets of analyses per day (i.e. 4 satellites, both day and night pass sets).

Validation against drifting and fixed buoy observations has shown that the standard deviation error of the instantaneous SST retrievals in this dataset is ~ 0.6°C. The magnitude of the bias error is less than 0.1°C (UO).

2.2 Pathfinder

The analysis reported here utilizes ascending and descending node "Best SST" equal angle projection data from the Jet Propulsion Laboratory Physical Oceanography Distributed Active Archive Center (PO.DAAC). These data have been retrieved from global area coverage AVHRR data, using a threshold based cloud detection algorithm and an NLSST retrieval algorithm where the first guess SST (used in the NLSST algorithm) is derived from the Reynolds optimally interpolated SST dataset.

The 1985 – 1990, and 1993 – 1999 data have been retrieved using the version 4.1 algorithm, while the version 3 algorithm was used for 1991 and 1992. The effective resolution of the Pathfinder (PF henceforth) data varies from 4.9 × 9.8 km at 60°S to 9.6 × 9.8 km at 10°S.

3 ANALYSIS METHODS

Monthly mean SSTs were estimated using mean-value temporal compositing. The mean value was set missing at any location where the temporal standard deviation exceeded 3°C or the sample size was less than 2. The data were then Cressman analyzed onto a common area and map projection (the NSA area), using a ~9 km grid for the NSA data, and an ~18 km grid for the PF data. The resulting monthly means were then expanded as a harmonic series, defined by the equation:

$$SST(x,t) = \overline{SST(x)} + \sum_{i=1}^{\frac{N}{2}} \left[A_{i,x} \cos(\omega_i t) + B_{i,x} \sin(\omega_i t) \right]$$

where N is the number of months in a year, ω_i is $2\pi\ i\ /\ N$, t is expressed in months, x is some location on the SST analysis grid, and the over-bar indicates the temporal mean. A linear regression technique is used to solve for the predictands ($A_{i,x}$ and $B_{i,x}$).

The spatial variability in the SST (gridded) analyses was decomposed by EOF analysis of the seasonal and monthly anomaly data, where seasonal anomalies were computed by removing the annual mean from each observation, and monthly anomalies by subtracting the monthly mean climatology. The temporal variability of the resulting EOF spatial patterns at seasonal and monthly timescales is

* *Corresponding author address:* Michael J. Uddstrom, NIWA, Private Bag 14 901, Kilbirnie, Wellington, New Zealand. Email: m.uddstrom@niwa.co.nz

referred to as the temporal amplitude here. The same approach was also applied to monthly spatial anomaly data, where each data sample is the monthly mean with its spatial mean removed. The usual naming convention is to call the EOFs computed from the seasonal and monthly anomaly data "temporal" EOFs, and those computed from the spatial anomaly data "spatial" EOFs. Borzelli and Ligi (1999) have shown that, neglecting vertical advection and assuming slowly time-varying horizontal advection, EOFs (multiplied by their temporal amplitudes) are particular solutions of the heat diffusion equation with advection, and that seasonal temporal, and spatial EOFs are equivalent. Accordingly, the domain over which the EOFs are computed will affect the resolved structures.

Given the evidence in Strong et al. (2000) and Casey and Cornillon (2001) for trends in SST in the NSA region, time series of water mass specific spatial averages at both annual (full field) and monthly (anomaly) time scales were estimated from both the NSA and PF datasets. These encompassed the East Australian Current (EAC), the Tasman Front, the Tasman Sea, SAW south of the CR, Subtropical Water (STW) north of the CR, as well as an area surrounding NZ. The same base climatology (NSA 1993–1997) was used for both sets of anomaly calculations.

4 RESULTS

4.1 Climatology

The NSA annual mean for the period 1993–2002 (inclusive) is shown in Fig. 1 Comparison of the 1993–1997 and 1993–2002 estimates shows the latter is, on average, 0.2°C warmer than the former – but the differences are not uniform. The EAC and Tasman Front regions were warmer during the first 5 year period, but the reverse is true for the Tasman Sea, while in the Subantarctic Water (SAW)east of NZ there is little difference between the two periods. However, over much of the rest of the domain, SSTs averaged over the 10 year period are ~0.2° warmer than those during the first 5 years.

Comparing the annual mean estimated from the PF data (1993–1997) with that from the NSA for the same period reveals what appears to be a latitude dependent difference. Except for areas adjacent to the coasts, the NSA mean SST is always warmer than that derived from the PF data, the difference being 0.05 - 0.1°C near 25°S, rising to ~0.3°C near 45°S, and 0.4 – 0.5°C south of 50°S.

4.2 EOF Analyses

The second spatial anomaly EOF (spEOF-2) pattern is shown in Fig. 2.

This pattern explains 28% of the residual variance after the first EOF (which has essentially the same structure as the annual mean) is removed. It is of particular interest because it clearly includes water-mass and frontal signatures (e.g. the EAC, Tasman Front (TF), East Auckland Current (EAuC), and Subantarctic Front, and seems to delineate the Tasman Sea from adjacent water masses. It also includes many of the features evident in the amplitude of the annual cycle (not shown here) such as the region of elevated variance in SAW south of the CR. The temporal amplitude for this EOF is shown in Fig. 3

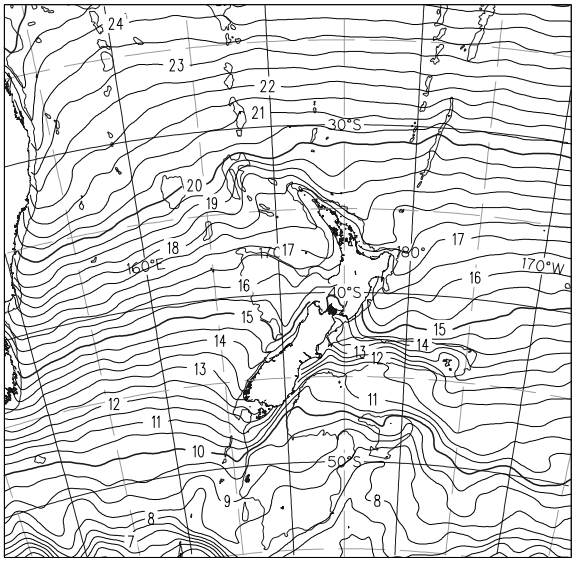

Fig. 1 NSA annual mean isotherms (0.5°C resolution). The bathymetry shown is that of the 1000 m isobath.

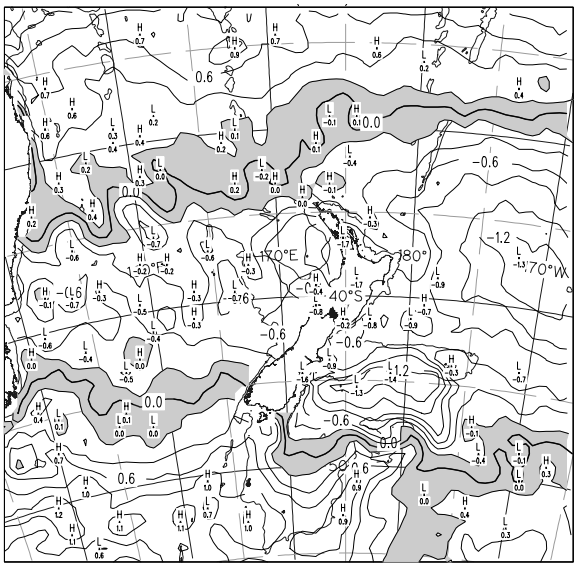

Fig. 2 Second spatial anomaly EOF (spEOF-2). The contour interval is 0.2, and values between ±0.2 are shaded. The bathymetry is indicated by the 1000m isobath.

The minimum in early 1998 occurred at the same time as the peak of the largest El Niño event of recent times, and one that resulted in positive SST anomalies in the New Zealand region, rather than the normal negative values. This event features in many of the EOF temporal amplitude series, but given the physical interpretation of features in Fig. 2 this EOF (and its temporal amplitude series) may suggest that

events in the Tasman Sea are of importance in explaining this anomalous event. This area of elevated SST also corresponds with the area of largest positive difference between the 1993–2002 and 1993–1997 NSA climatological annual means noted above.

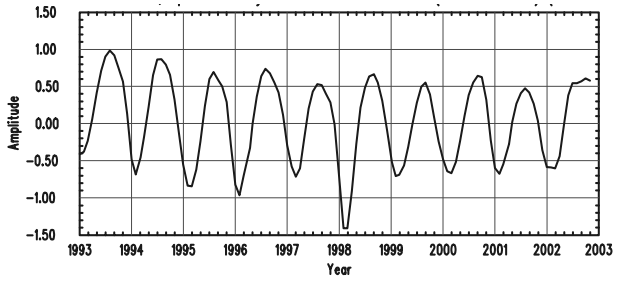

Fig. 3 Temporal amplitude of sp EOF-2 (1993 – 2002), using the 1993 – 2002 climatology.

4.3 Trends

PF and NSA monthly anomaly spatial means for STW and SAW water masses east of NZ are shown in Fig. 4. These results typically show large month to month changes – probably due to changes in surface wind stress and hence vertical mixing – superimposed on a lower frequency ENSO signal However, more importantly, while the PF and NSA data are in quite good agreement for the STW domain, this is not the case for the SAW domain. The PF data indicate a warming between 1993 and 1999, but the NSA data show no similar "trend". This difference appears unrelated to sample size, as both datasets have nearly identical sample sizes (~20000 each month), and the standard error of the estimate is typically 0.02°C.

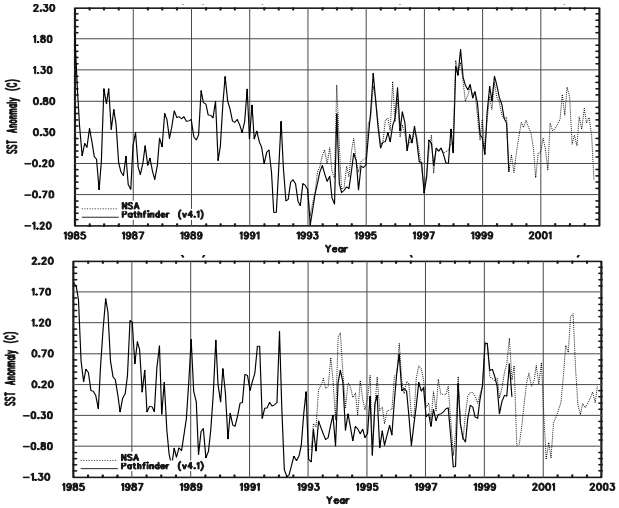

Fig. 4 Water mass-specific monthly anomaly spatial means for STW (top) and SAW water masses east of NZ. The NSA data are shown with a dotted line.

5 DISCUSSION

A striking observation resulting from this work is that all of the features identified in the UO 5 year (1993-1997) climatology and spatial variance analysis are also found in the 10 year (1993–2002) analysis. Examples include; the positions of meanders in the TF, the wavelike features in the isotherms over, and east of the Kermadec Ridge, the permanent positions of meanders in the SAF south and east of NZ, and the position of the STF beyond the Chatham Islands. Although not shown here all of these features , remarkably, can also be identified in the 15 year (1985–1999) PF climatology. Given the independence of the cloud detection and SST retrieval algorithms employed in each dataset, this result provides good evidence for the usefulness of SST time series data to describe spatial and temporal variability of significant ocean features in the region.

With regard to STW south of the CR; recently *in situ* measurements have observed at least one feature largely made up of STW at 50°S, 172°W (Williams, 2002). This position is very close to the location of the STF proposed by UO.

The results reported here also underline the uncertainties involved in simple trend analyses. For example, two adjacent water masses (SAW, and STW, east of NZ) display quite different responses to climate events. There is evidence for a large annual cycle in the anomalies in SAW, but no similar periodicity is evident in the STW to the north. Also, while the STW low frequency variability reflects that of the SOI, that of the SAW water mass is more complex. Further, while the PF data indicate a warming trend ($0.20\pm0.02°Cy^{-1}$) in SAW after 1993, the equivalent period in the NSA data record indicates a much smaller trend ($0.02\pm0.02°Cy^{-1}$). In the EAC water mass the PF data show a warming trend ($0.02\pm0.008°Cy^{-1}$) over the period (1985-1999), similar to that reported in Casey and Cornillon (2001), but the NSA record indicates cooling ($-0.005\pm0.01°Cy^{-1}$).

Clearly, high-resolution SST data have the potential to provide useful new information about the ocean environment – but interpretation is challenging.

References

Borzelli, G. and Ligi, R. (1999) Empirical orthogonal function analysis of SST image series: A physical interpretation. *J. Atmos. Ocean. Tech.* **16:**682-690.

Casey, K.S., and P. Cornillon, 2001: Global and regional sea surface temperature trends. *J. Climate.* **14**, 3801 – 3818.

Strong, A.E., E.J. Kearns, and K. K. Gjovig, 2000: Sea surface temperature signals from satellites - an update. *Geophys. Res. Letters* **27**, 1667 – 1670.

Uddstrom, M.J., Gray, W.R., Murphy, R., Oien, N.A. and Murray, T., 1999: A Bayesian cloud mask for sea surface temperature retrieval. *J. Atmos. Ocean. Tech.* **16:**117-132.

Uddstrom, M.J. and Oien, N.A., 1999: On the use of high resolution satellite data to describe the spatial and temporal variability of sea surface temperatures in the New Zealand Region. *J. Geophys. Res.-Oceans* **104(C9):**20729-20751.

Williams, M.J.M., 2002: Analysis of quasi-synoptic eddy observations in the New Zealand Subantarctic. Submitted to *N.Z. J. Mar. Fresh. Res.*